Chapter 2

Experimental Techniques and Analysis Methods

2.1 Introduction

To investigate the nuclear structure at high spin, special techniques are needed. In this chapter, we will discuss about the methods of populating high-spin nuclei and experimental setups that are used to produce high-spin nuclei and detect the de-excited γ-rays emitted from a particular nucleus.

2.2 Population of High Spin Nuclei with Fusion Evaporation Reaction

Numerous techniques have been developed for producing nuclei with high angular momentum. The heavy ion-induced fusion-evaporation reaction is the most effective technique among them. In this method, the accelerated projectile particle having energy greater than the Coulomb barrier of the target and projectile nuclei collides and fuses with the target

nucleus. After the fusion process, a compound nucleus is formed within a short time of

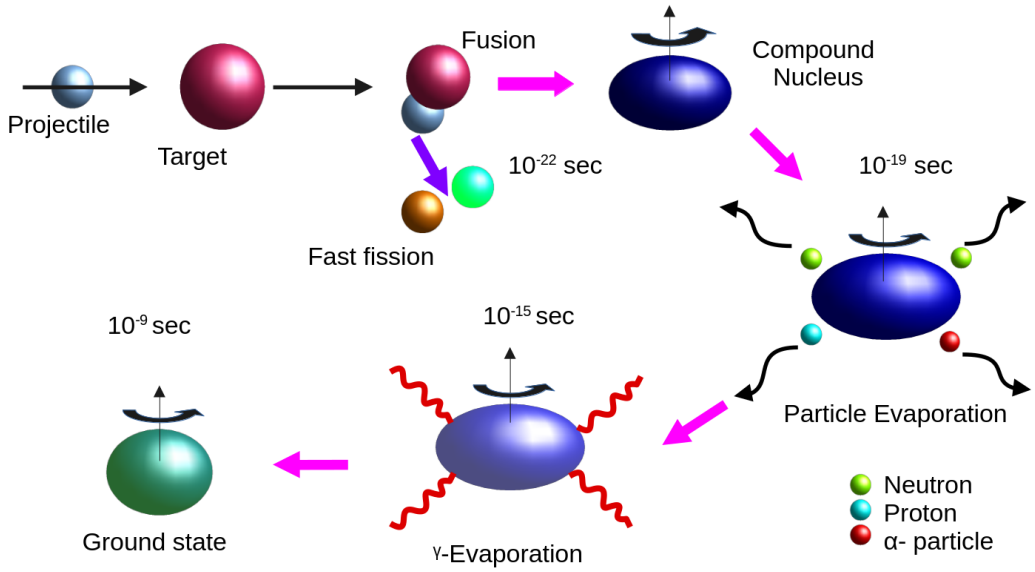

Figure 2.1 Schematic diagram illustrating the various modes of formation and decay of a compound nucleus.

10^{-22} to 10^{-20} sec.

The compound nucleus is a very hot and fast-rotating object that initially cools down by particle evaporation (neutron, proton, or particles) $\sim 10^{-16}$ sec. Since the neutron evaporation process is unaffected by the Coulomb barrier, the emission of neutrons is preferred. On the other hand, protons and alphas are charged particles, their evaporation are hindered by the Coulomb barrier. The coulomb barrier energy and excitation energy of the compound nucleus are defined as:

$$V_{coul} = \frac{(A_P + A_T)}{A_T} \frac{1.44 Z_P Z_T}{1.2(A_P^{1/3} + A_T^{1/3} + 2)}, \tag{2.1}$$

$$E_{exc} = \frac{A_T}{A_T + A_P} E_{projectile} + Q, \tag{2.2}$$

where A and Z represent mass and atomic number, while subscripts P and T denote the projectile and target, respectively. Q is the energy released as a result of the difference

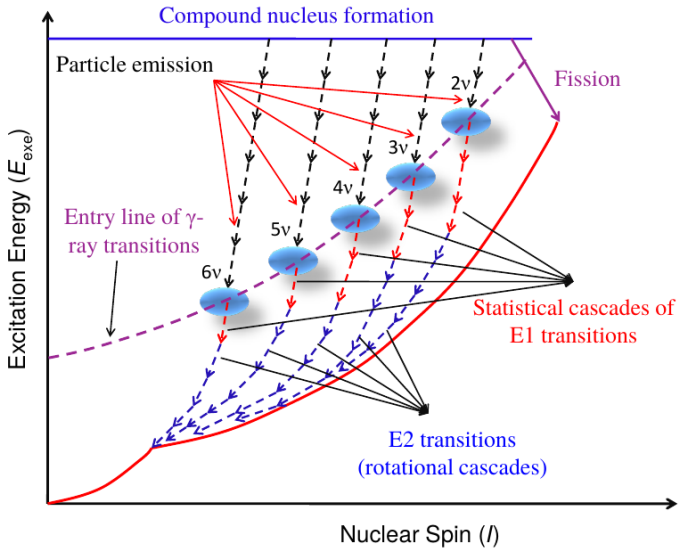

Figure 2.2 Excitation energy as a function of spin for the decay of the compound nucleus in a heavy-ion-induced fusion-evaporation reaction. The Figure is taken from Ref. [71]

.

between the final and initial masses, and $E_{projectile}$ is the projectile's kinetic energy. It is possible to determine the compound system's maximum angular momentum as follows:

$$l_{max}^2 = \frac{2\mu R^2}{\hbar^2}(E_{cm} - V_{coul(cm)}), \tag{2.3}$$

where μ is the reduced mass of the system, given by $\mu = \frac{A_T A_P}{A_T + A_P}$. The R represents the recoiled distance of the closest approach and may be approximated as the sum of the radii of the projectile (R_P) and target (R_T). The entire process of compound nucleus formation is represented by the above sets of equations, which were first suggested by Niels Bohr [72] and later on experimentally verified by S. N. Ghoshal [73].

Particle evaporation will continue until the excitation energy remaining in the system is within a nucleon binding energy (8 MeV). After this point, particle evaporation is no longer energetically possible, and the nucleus decays via γ-ray emission. After the subsequent emission of particles and statistical γ rays, the residual nucleus enters into

the yrast line, which is the line of the lowest energy for a specific angular momentum. Formation and the de-excitation mechanisms of the compound nucleus have been shown in Figs. 2.1 and 2.2.

In a heavy-ion reaction, the residual nuclei are aligned with their spin direction in a plane perpendicular to the beam axis. This is helpful in determining the multipolarity of γ rays. Several packages like PACE4 [74] and CASCADE [75] are available for calculating theoretical fusion-evaporation cross-sections in reactions.

2.3 γ-Ray Detection

In a fusion-evaporation reaction, the compound nucleus, in an excited state below the particle separation threshold, decays predominantly through the emission of γ rays until it reaches to the ground state. Detecting the gamma rays emitted from excited nuclei helps determine the nuclear energy levels. To measure the energy of gamma rays in a detector, γ rays need to lose energy within the detector material. There are three main ways through which gamma rays interact with matter: Photoelectric effect, Compton Scattering, and Pair Production.

2.3.1 Photoelectric Effect

In this process, complete absorption of γ-rays occurs within the material, and it emits a bound electron with energy E_e. A small part of the incident γ energy is used to overcome the electron binding energy, whereas the rest is transferred to the free electron as kinetic energy.

$$E_e = E_\gamma - E_B. \tag{2.4}$$

Where E_γ is the γ-ray energy and E_B is the electron binding energy.

The cross-section of the photoelectric effect (σ_{photo}) for a typical HPGe detector varies as

$$\sigma_p \propto \frac{Z^n}{E_\gamma^{3.5}}. \tag{2.5}$$

where N varies from 3 to 5 and Z is the atomic number of the detector. The dependence of these interaction processes on the γ-ray energy is shown in Fig. 2.3

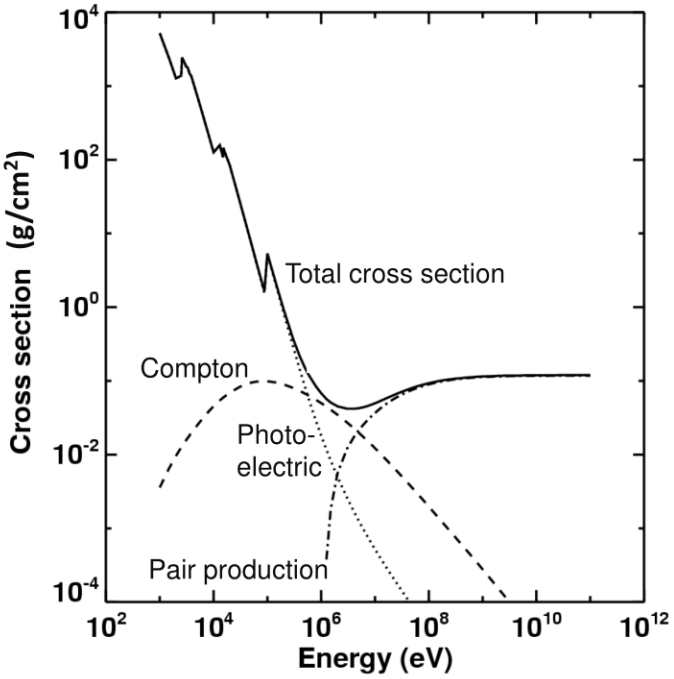

Figure 2.3 The energy dependence of the various gamma-ray interaction processes [71].

2.3.2 Compton Scattering

Compton scattering occurs when an incident γ-ray photon is scattered by a free or weakly bound electron, transferring some of its energy to the electron. The scattered photon's energy can be calculated using the energy and momentum conservation relations as follows:

$$E'_\gamma = \frac{E_\gamma}{1 + (1 - \cos\theta)\frac{E_\gamma}{m_0 c^2}}, \tag{2.6}$$

Where E'_γ, E_γ, and θ represent the energy of the scattered photon, energy of the incident photon, and scattering angle between the incident photon and scattered photon. m_0c^2 is the rest mass energy of electron. The kinetic energy of the electron is given by,

$$E_e = E_\gamma - E'_\gamma = \frac{E_\gamma^2(1-cos\theta)}{m_0c^2 + E_\gamma(1-\cos\theta)} \tag{2.7}$$

The maximum energy transfer to the electron happens when the γ-ray photon is scattered at an angle θ = 180°. It can be seen that a continuum of energies can be transferred to the electron, ranging from θ = 0° to θ = 180°. The γ-ray photon never loses all of its energy during this process. A constant "Compton background" consequently develops at lower energy levels in the energy spectrum.

The Compton-scattering cross-section is approximated to be:

$$\sigma_c \propto \frac{Z}{E_\gamma}. \tag{2.8}$$

The effect is dominant for γ rays with intermediate energy, as shown in Fig. 2.3.

2.3.3 Pair Production

Pair production takes place when the incident γ-ray with energy greater than or equal to twice the rest mass energy of the electron ($E_\gamma \geq 1.022$ MeV) passes through the strong field of the nucleus. The nucleus receives a very small amount of recoil energy to conserve the linear momentum. A positron immediately annihilates with the surrounding electron and produces two photons with equal energy. When one of the annihilated gamma rays enters into detector, it results in a peak located at 0.511 MeV. The probability of pair production approximately varies with the square of the Z.

A γ-ray detector must have high efficiency to ensure high statistics and high resolution to distinguish γ-rays that are close in energy. Semiconductor detectors made of High-Purity

Germanium (HPGe) crystals offer outstanding energy resolution but low detection efficiency, whereas scintillation detectors made of Sodium Iodide (NaI) or Bismuth Germanate ($Bi_4\ Ge_3\ O_{12}$)(BGO) have high efficiency but poor energy resolution. However, the time resolution of the HPGe detector (10 ns) is lower than that of scintillator detectors. For better results, a combination of both semiconductor and scintillation detectors is used in spectroscopic studies.

2.4 HPGe Detector

The operation of the high-purity germanium detectors is identical to that of reverse-bias p-n junction semiconductor detectors. The important parameter of the detector is active volume, which is determined by the thickness of the depletion region. γ-ray spectroscopy requires detectors with much larger depletion depths. The depletion depth for a semiconductor detector is determined by

$$d = \left(\frac{2\varepsilon V}{eN}\right)^{1/2} \tag{2.9}$$

where V is the reverse bias voltage, N represents the net impurity concentration, ε is the dielectric constant, and e is the electronic charge. If we use germanium in its natural form, then the maximum achievable depletion depth is only a few mm, which is not suitable for γ-ray spectroscopy. The impurity concentration should be reduced down up to 1 part in 10^{12} in order to get the depletion region of the order of a few cm.

The n-type detectors are generally preferred because they are less susceptible to neutron damage and they have the ability to detect low-energy transitions due to their thinner contacts. HPGe detector has an excellent energy resolution ($\sim$ 2 keV at 1 MeV) compared with gas detectors or scintillators. The energy resolution is better in a germanium detector because only $\sim$ 3 eV energy is required to create one electron-hole pair. In order to reduce thermal electronic noise, HPGe detectors operate at liquid nitrogen temperature (77 K).

Unlike Ge(Li) or Si(Li) detectors, these detectors need not always be kept at liquid nitrogen temperature when not in use.

2.5 BGO Detector

Despite having a good resolution, HPGe detectors are not very efficient. As described above, various interactions can occur when a γ-ray enters in the detector. Due to the limited detector size, many of the γ-rays will Compton scatter and escape, resulting in an incomplete energy deposit. Only γ-rays that deposit their entire energy in the detector allow for accurate measurement of γ-ray energy. The Compton scattering of many γ-rays are responsible for the background in the spectrum, thereby reducing the peak-to-total ratio. Peak-to-total ratio (PT) for a detector is defined as:

$$PT = \frac{Total\ number\ of\ counts\ in\ photopeak}{Total\ number\ of\ counts\ in\ entire\ spectrum} \tag{2.10}$$

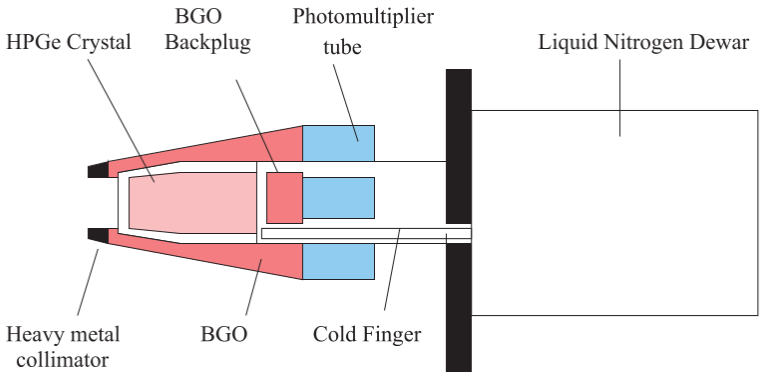

Figure 2.4 Schematic diagram of an escape-suppressed HPGe detector as used in the Gammasphere array [76].

.

One solution to the issue is to remove the Compton component by enclosing each HPGe detector with an anti-Compton shield (ACS). Generally, BGO detectors are used as

a Compton shield because of their high density and atomic number, resulting in the highest γ-ray absorption coefficient per unit size of scintillator material. Fig. 2.4 represents the schematic diagram of a HPGe detector surrounded by BGO detectors. The events detected in the detector and the shield simultaneously can be rejected electronically, which provides a veto for Compton-scattered events. A stand-alone HPGe detector has a peak-to-total ratio of 20%. This configuration improves the peak-to-total by around 50-60%.

2.6 Clover Detector

The size of the detector plays an important role in increasing the detector efficiency. A larger detector offers higher detection efficiency, but the wider solid angle causes significant Doppler broadening of the recorded γ-rays, consequently reducing the energy resolution. Also, growing a large single crystal involves experimental constraints. An economical way to evade this problem is to mount more than one small Ge crystal (110 cm^3) side by side within the same cryostat surrounded by the common ACS. The clover detector is a type of composite γ-ray detector that consists of four n-type coaxial high-purity germanium (HPGe) crystals that are mounted in a common cryostat to form a structure. Each crystal has a typical diameter of 46 mm and a length of 70 mm. The total active volume of a clover detector is $\sim$ 470 cm^3, which is about 89% of the total volume. A schematic diagram of a clover detector is shown in Fig. 2.5.

The front face of the crystal is shaped in quasi-square, which enables a close packing with a minimum Ge-Ge distance of about 0.2 mm. The advantage of the clover detector with respect to a single HPGe detector is discussed below:

• In a clover detector, the effective solid angle is reduced for individual crystals of clover, which improves the energy resolution.

• The small size of a single crystal improves the timing characteristics much better than that of a single large HPGe detector.

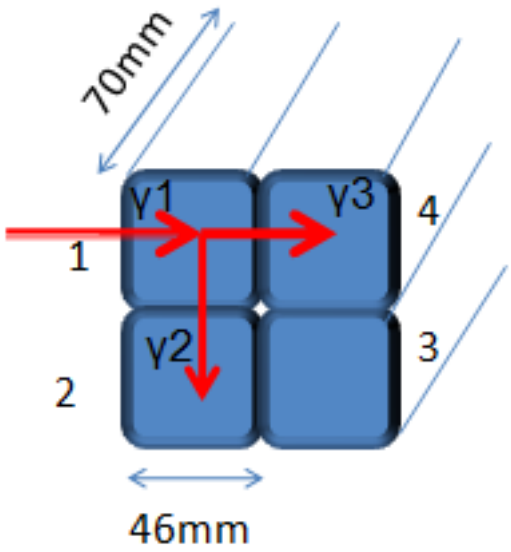

Figure 2.5 Schematic diagram of clover detector.

• The small opening angle of a single crystal reduces the effect of Doppler broadening on the resulting spectra.

• The use of clover enables recovery of the lost photopeak energy due to Compton scattering by a time-correlated addition of energy signal in all four crystals. The mode is known as the Addback mode. This increases the overall peak-to-total ratio of the clover detector.

• The clover detectors can also be used as a polarimeter, where each of the individual crystals can be considered as a scatterer and the two adjacent detectors as the absorbers. Since the Compton scattering is preferential along the horizontal and vertical directions with respect to the reaction plane for the magnetic and the electric type of transitions, respectively. Thus, the electric or magnetic nature of the incident γ-ray can be determined by comparing the efficiency-corrected intensities of "Addback" lines from the horizontal and vertical scatters.

2.7 Multi-Detector Arrays

The advantage of using a multidetector array over a single High Purity Germanium (HPGe) detector improves the overall performance of gamma spectroscopy systems. With the help of a multidetector array consisting of N Compton-suppressed HPGe detectors, the number of two-fold events can be increased by a factor of $N(N-1)/2$. A multidetector array can cover a larger solid angle compared to a single HPGe detector, improving the efficiency of detecting gamma rays. This results in higher overall counting rates and better sensitivity to weak signals. By using an extensive array of detectors, gamma photons emitted from various directions can be detected simultaneously, which are helpful in determining the multipolarity of gamma transitions.

2.8 Resolving Power

The resolving power (R_p) of an array is the measure of its effectiveness in resolving sequences of γ transitions from a very complex spectrum. It is given by [77]:

$$R_p = (SE_\gamma/\Delta E_\gamma)PT \tag{2.11}$$

where SE_γ is the average energy separation between two transitions in a cascade. PT refers peak-to-total ratio. The energy resolution $\Delta {E_\gamma}^2$ of a detector is expressed as [77] :

$$\Delta {E_\gamma}^2 = (\Delta {E_{int}}^2 + \Delta {E_{open}}^2 + \Delta {E_{ang}}^2 + \Delta {E_{vel}}^2). \tag{2.12}$$

where ΔE_{int} is the intrinsic resolution of the detector whereas ΔE_{open}, ΔE_{ang} and ΔE_{vel} represent the effect of Doppler broadening on resolution due to opening angle of detector, angular spread of the recoil nuclei in the target and due to spread in velocity of recoiling nuclei, respectively.

2.9 Gammasphere Array

The Gammasphere Array at Argonne National Laboratory is a sophisticated setup designed to provide high-resolution gamma-ray spectroscopy for nuclear physics experiments [78]. The array was comprised n-type Ge detectors with a BGO Compton suppressor shield in 4π symmetry. Enhanced efficiency was achieved by using large-volume n-type Ge detectors. The diameter of a detector is 7 cm, while it is 7.5 cm long. The system consists of 110 functional detectors. The front 2 cm of the Ge detector is tapered with a half angle of 7.45°. The target-to-detector distance is 24.6 cm. The length of the BGO element is 18 cm, and the distance between its surface to the target is 21.8 cm. Detectors are bunched in groups of 5 to 10 detectors each and are mounted symmetrically at 17 different orientations with respect to the beam direction. In Fig. 2.6 Gammasphere array is shown. The photopeak efficiency for 1.33 MeV peak of ^{60}Co is $\sim 9.9\%$ with fully working 110 detectors, while a P/T ratio of 60% and an energy resolution of 2.5 keV have been achieved [78]. 70 crystals were electronically separated into two semi-circular D-shaped segments from a total of 110 detectors. This arrangement reduces the opening angle to almost half, thereby reducing the Doppler broadening. Fig. 2.7 shows a schematic illustration of segmented Ge detectors. Mounting these detectors at 90° enhances energy resolution and makes polarization measurements easier [79].

2.10 Indian National Gamma Array (INGA)

The Indian National Gamma Array (INGA) is a multi-detector array, a setup in collaboration with the Tata Institute of Fundamental Research (TIFR), Inter-University Accelerator Center (IUAC), Bhabha Atomic Research Centre (BARC), Saha Institute of Nuclear Physics (SINP), Variable Energy Cyclotron Centre (VECC), UGC DAE Consortium for Scientific Research, and many Universities in India. In the present thesis, the INGA

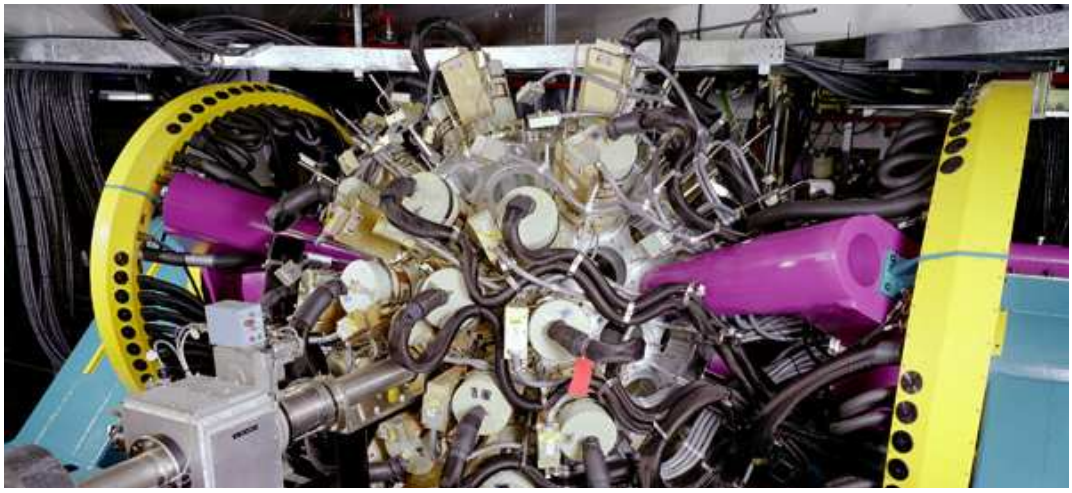

Figure 2.6 Schematic diagram of a view of the Gammasphere spectrometer. Figure taken from Ref. [76].

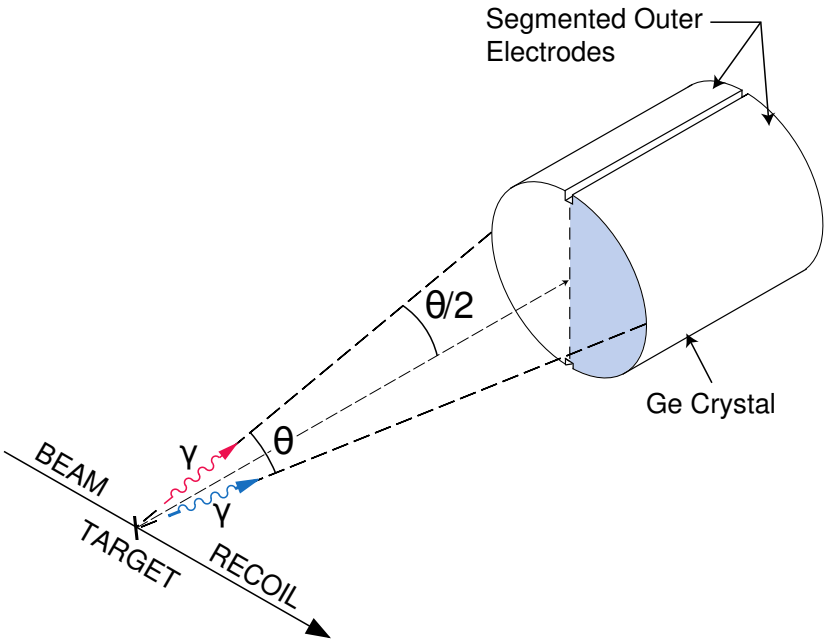

Figure 2.7 Schematic representation of segmented Ge detectors. Figure taken from Ref. [76].

Figure 2.8 INGA set up at T.I.F.R. Mumbai (left panel) and VECC Kolkata (right panel).

installed at TIFR and VECC was used to study the structure of ^{119}I and ^{114}Te, respectively.

The INGA setup at T.I.F.R.-Mumbai consists of a maximum of 24 clover detector slots, and it has 4π symmetry. Twenty-four clover detectors are arranged at six different azimuthal angles, with four detectors at 90° and three detectors at each 23°, 40°, 65°, 115°, 140°, and 157°. The distance between the target and detector in this setup is ∼25 cm. The maximum photopeak efficiency of ∼5% can be achieved with this array. In the addback mode, the array has a peak-to-total ratio of 40% and FWHM of ∼2.2 keV for the 1.33 MeV γ-ray of ^{60}Co. Fig. 2.8 shows the schematic diagram of TIFR-INGA. The preamplifier of each of the 4 crystals has a gain of 200 mV/MeV, and the decay time constant of the output is 50 μsec.

The array at VECC comprised Compton-suppressed HPGe (High Purity Germanium) clover detectors, placed at three different angles with respect to the beam direction. Fig. 2.8 shows the experimental setup of the INGA at VECC, Kolkata. There were ten slots available for mounting detectors. Seven HPGe clovers and one LEPS (Low Energy Photon Spectrometer) were used in one of our experiments. Four of the clover detectors were

positioned at 90°, two at 125° (backward angle), and one at 40° (forward angle) with respect to the beam direction. The LEPS detector was used to capture the low-energy photons and was placed at 40°.

2.11 Signal Processing

The working of conventional signal processing involves analog hardware. The pre-amplifier receives the signals from the detectors and extracts two identical signal pulses from each detector, one of which can be used to determine at which time the energy is deposited and the other to determine the amount of energy deposited. The pre-amplifier then sends the pulses through the amplifier. Distortion effects like *walk* and $time - jitter$ are produced within the original signal. $Constant\ fraction\ discriminator$ or CFD is used to remove *walk*. A variety of filters with a small time constant are used to optimize the pulse signal, producing a pulse with a very short rise and fall duration. This improves time definition and lowers the noise factor. After these modules, *coincidence unit* (CU), comes next. The CU is used to set the width of the coincidence window. The two gamma quanta are considered to be emitted promptly if they arrive inside this time range or interval. Although a quick emission of two gamma quanta should ideally provide simultaneous time signals from each detector, jitter reduces this time, resulting in the loss of certain coincident gamma pairs. Similar to a typical AND gate, CU will produce a logic pulse when both of its input signals are active.

2.11.1 Data Acquisition (DAQ) System of Gammasphere

The Gammasphere electronics comprised amplifiers, discriminators, and *ADC*s, all housed in VXI modules. Analog time and energy signals produced as detector outputs are pre-amplified and then amplified in amplifier modules. The output signal from the amplifier is

digitized by *ADC*s. The whole process is completed within a time duration of $\sim 10\mu$s. The processing of BGO detector signals is the same as that of the HPGe detector. The signals coming from the HPGe and BGO detectors are transferred to a logic board to suppress the Compton scattering. Three sets of triggering mechanisms are used in the data acquisition system, which receives signals from all 110 detectors. In the first trigger mechanism, four or more Ge detectors should be fired simultaneously within a time interval of 200–800 nanoseconds. The next one with a 1μs time limit will ensure that at least three detectors fire even after Compton suppression. The last time window of 6μs is kept for pile-up rejection. The system will automatically reset in 1μs if any of the above-mentioned requirements are not met; otherwise, the acquisition system will read out all relevant data [80–82]. A schematic diagram of the experimental set-up is shown in Fig. 2.9.

2.11.2 Data Acquisition (DAQ) System of TIFR-INGA

In order to collect the energy and timing information for all 96 channels of the 24 clovers vetoed with the respective Compton-suppressed BGO shields, a digital data acquisition system has been used with the INGA setup. The DDAQ interfaces with high-capacity storage systems to handle the large volumes of data generated by INGA. The DDAQ has six Pixie-16 modules, two LVDS level translator modules, and one controller arranged in a single Compact PCI/PXI crate as depicted in Fig. 2.10. Each Pixie-16 module has sixteen channels and serves four clover detectors. The preamplifier signals coming from all the clover detectors are digitized with a 12-bit 100 MHz Flash Analog to Digital Converter (FADC). Before applying the input signals to the DDA, each signal is processed in the analog circuitry to compensate for the DC offset and remove the high-frequency component of the signals.

The digitized data of the incoming analog pulse enters in the signal processing circuit. This data stream is fed into two branches. The first branch generates a trigger through

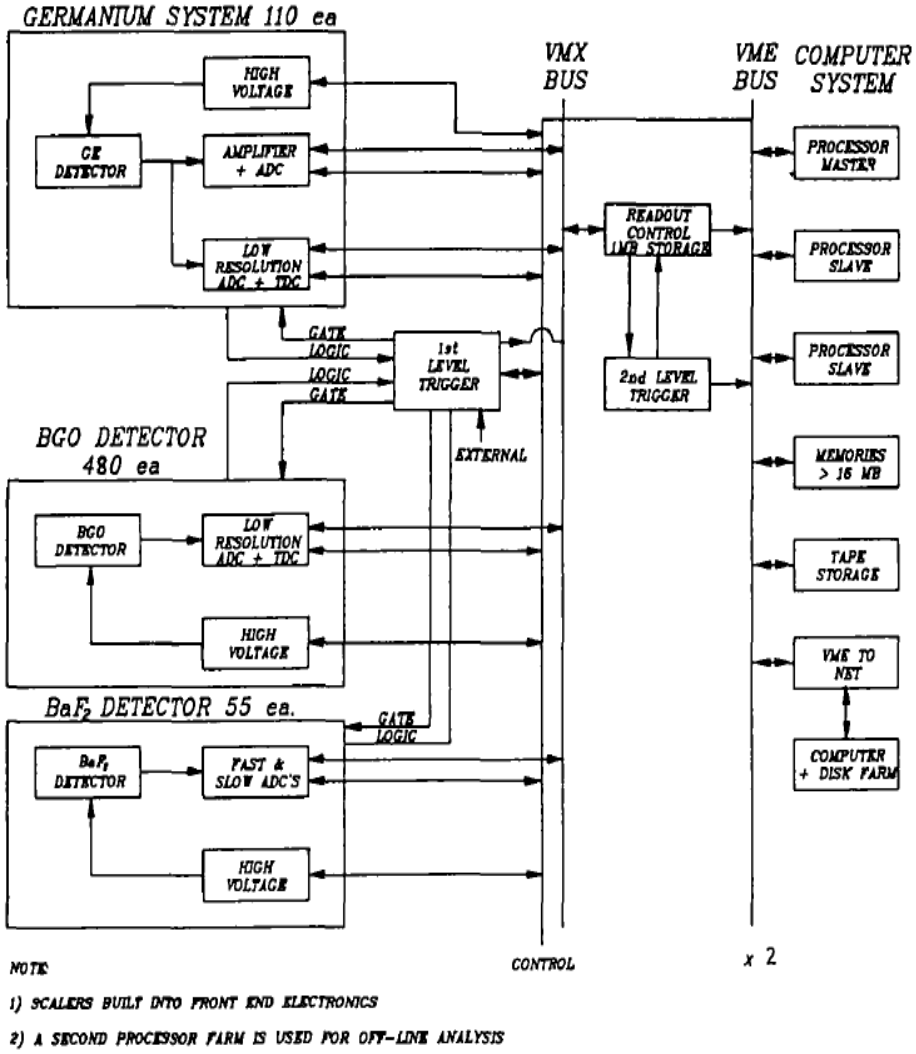

Figure 2.9 Schematic representation of the experimental set-up of Gammasphere array. Figure taken from Ref. [78].

a fast trapezoid filter for total multiplicity computation in the onboard FPGA. The fast trigger is generated when the output of the digitizer data crosses the defined threshold. Through the PXI back-plane, the fast triggers produced by any of the 16 channels of the Pixie-16 module can be transferred to other modules for the generation of global triggers. The trapezoidal filter was stretched to a 100 ns pulse width and was created for the purpose of creating multiplicity groups. In the second branch, after passing data through a delay FIFO, the data is further split into a trigger filter for fast trigger detection for local signal processing (such as a pile-up detector) and an energy filter for data sampling. In the current design, one of the six cards in a single crate, named Director, receives and distributes triggers to all channels. The director computes the multiplicity and opens a coincidence window of a specified length.

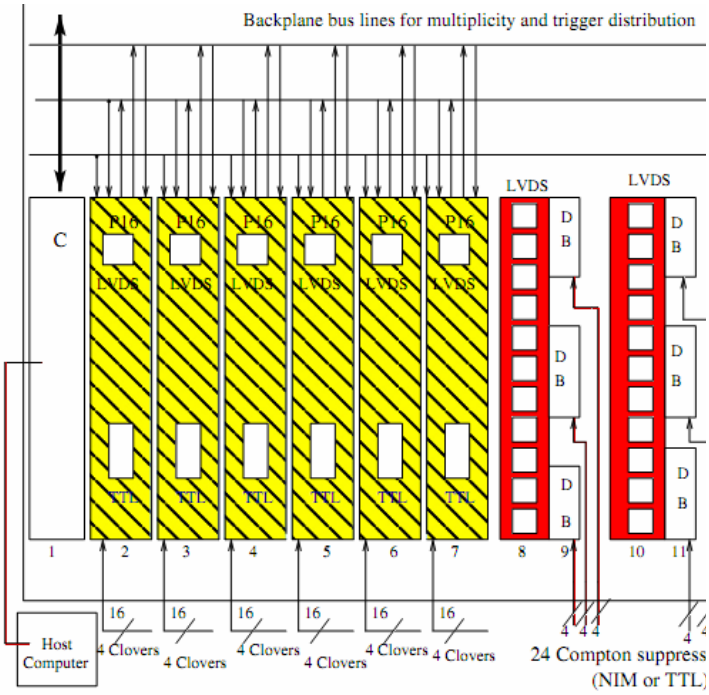

Figure 2.10 Block diagram of Pixie-16 module. Figure taken from Ref. [83].

A logic signal is generated through conventional fast trigger circuits using *TFA* and *CFD* for BGO detectors. The signal is in turn fed to Pixie-16 modules for veto. When

no veto signal is present, a rapid trigger generates a valid signal. For each valid signal from the preamplifier, energy information is collected using on-board digital pulse shape processing, and timing is measured by latching the clock with the arriving pulse. The crate is connected to a PC through an optical bridge. The data acquisition is monitored by a PC, which searches for FIFO (first in, first out) in each module. When the FIFO is ready, the data is transferred to the PC. All of the modules in the digital system are synced according to the precision defined by the clock. Following that, the list mode data for each module is written to distinct files on the hard disk. The time-stamped data from various Pixie modules was combined into a single data stream in offline mode. The data sorting code, MultipARameter time-stamped based COincidence Search program (MARCOS) [83] developed at the Tata Institute of Fundamental Research (TIFR), was used to sort the time-stamped combined data.

2.11.3 Data Acquisition (DAQ) System of VECC-INGA

A digital data acquisition (DDAQ) system is used to process signals and collect data. The data was stored by a 12-bit, 250-MHz PIXIE 16-digitizer-based system manufactured by XIA LLC, USA. The time-stamped list mode data is acquired with the event multiplicity M_γ = 1 for singles and 2 (for coincidence). Once a specific event is recorded corresponding to a particular channel, the digitizer writes 32-bit words containing the information regarding the channel number (detector ID), timestamp, CFD value, the energy of the recorded pulse, and a flag for the pile-up events. The 93% of the collected data were found to be two-fold, while the rest were three and higher fold. The DDAQ was facilitated by the UGC-DAE CSR, Kolkata Centre [84]. The data obtained in raw form were processed and sorted into several symmetric and asymmetric $\gamma-\gamma$ matrices and $\gamma-\gamma-\gamma$ cubes by the IUCPIX package developed by UGC-DAE-CSR, Kolkata Centre [84].

2.12 Data Processing

The data acquired from the fusion-evaporation reactions are analyzed in offline mode. The offline data analysis can be divided into two parts: (a) pre-sorting of data, which includes gain matching, energy and efficiency calibrations, add-back method, etc. (b) Data compression, which comprises LIST mode data and has a size smaller than the raw data. The list mode data contains information of γ-ray energies, timing information of the arrival of photons, and multiplicity.

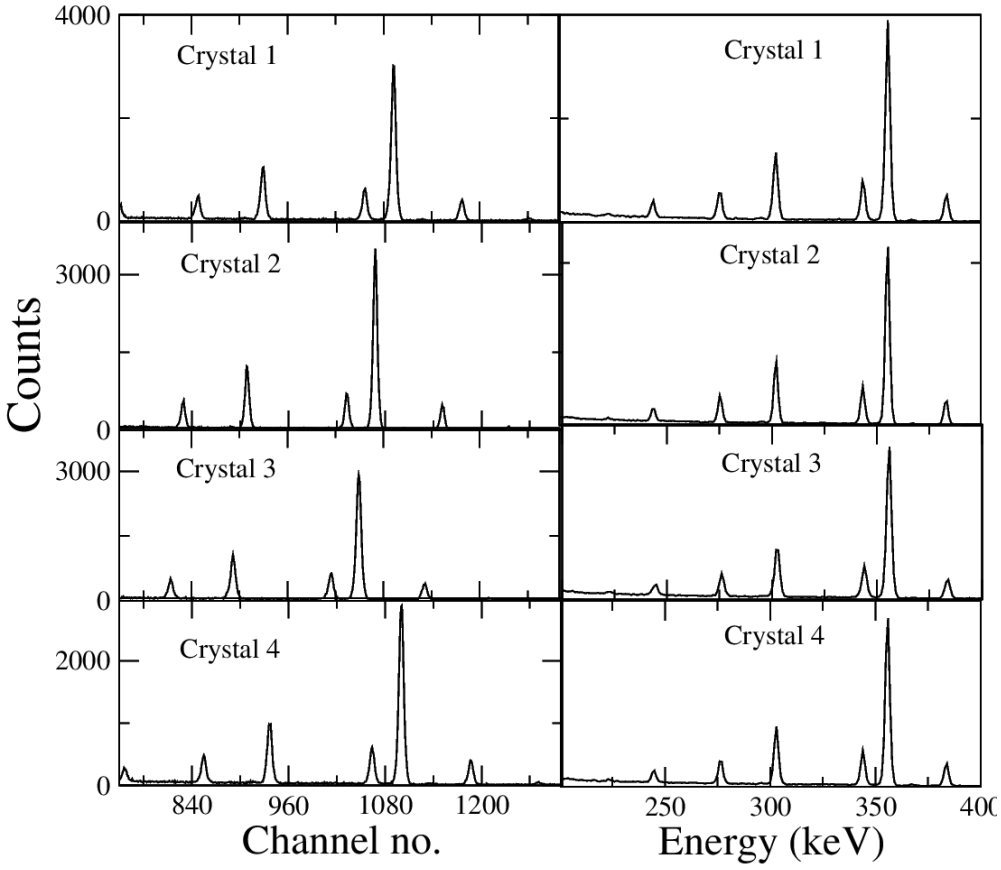

Figure 2.11 The effect of both energy calibration and gain matching is shown for all the crystals of a clover detector.

2.12.1 Gain-Matching

The different detectors tend to have varied amplification factors for the received signals. Even in the case of the clover detector, signals recorded from all four crystals are at different positions. This is generally termed as gain, and to obtain the add-back spectra, each crystal has to be gain-matched, because during the addback process, the spectra generated from each crystal of clover are added up channel-wise which results in broadening of photopeak without gain-matching. For each detector, a set of correction coefficients are evaluated and used for the add-back process. In the addback process, the time-correlated signals from two neighboring segments (horizontal or vertical) are added. On the other hand, the signals that hit in two diagonal segments are discarded. Furthermore, the gain is not stable over the time span of long-term experiments. Electronic instability may cause changes in gain for detectors and crystals. As a result, it is recommended to match the gain parameters of detectors/crystals with a set of data acquired over various time intervals throughout the experiment. The process can be implemented either online, as in Gammasphere [78], or offline, as in INGA. In Fig. 2.11, the gain matching of a clover detector is depicted.

2.12.2 Energy Calibration

Energy calibration is an essential requirement to gain matching. At a given high voltage, the gain factors for the various crystals vary. After digitization, voltage pulses for specific γ-ray energies have different ADC channel numbers. In order to know the exact energy values, energy calibration is done by using standard radioactive sources ^{152}Eu and ^{133}Ba at target positions. The centroid of each peak is defined by the channel number in the detector/crystal, and the known energies are matched to the channel numbers using a polynomial fit based on:

$$E_\gamma = \sum_{n=1}^{k} (a_0 + a_n x^n). \tag{2.13}$$

where x's are the channel numbers for the known energies E_γ. a_n and n are the calibration coefficients and the degree of the polynomial, respectively. The coefficient "a_0" basically gives the offset value. The first-order coefficient gives an idea about the gain of the amplifier, whereas the second-order coefficient measures the non-linearity in the detection setup.

2.12.3 Efficiency Calibration

Each detector/crystal has a unique efficiency characteristic, which determines how many photons are detected relative to those emitted by the source or incident on the detector. As a result, in order to assess the relative intensities of the observed transitions, efficiency correction must be applied across the detector setup. For this purpose, known sources with properly measured relative intensities are used to compare the relative intensities in the given system. The experimental data points are fitted by a theoretical function, using the RADWARE package [85], which is expressed as:

$$ln(\varepsilon) = [(A + Bx + Cx^2)^{-G} + (D + Ey + Fy^2)^{-G}]^{-1/G}. \tag{2.14}$$

where, ε is the efficiency, x = ln(E_γ/100) and y = ln(E_γ /1000). The γ-ray energy E_γ is in keV. The parameters A, B, and C describe the lower energy efficiency, whereas D, E, and F govern the behavior of the high energy part of the efficiency curve. The interaction parameter G determines the shape of the turnover region between the efficiency curve's higher and lower energy parts. The total efficiency vs E_γ plot calculated for the INGA setup of TIFR Mumbai is shown in Fig. 2.12.

The addback efficiency at higher energy is greater than that obtained without addback because Compton scattering is more prominent at higher energies. The add-back factor is defined as the ratio of a clover detector's detection efficiency to the time-uncorrelated sum of the detection efficiency of its four independent single crystals.

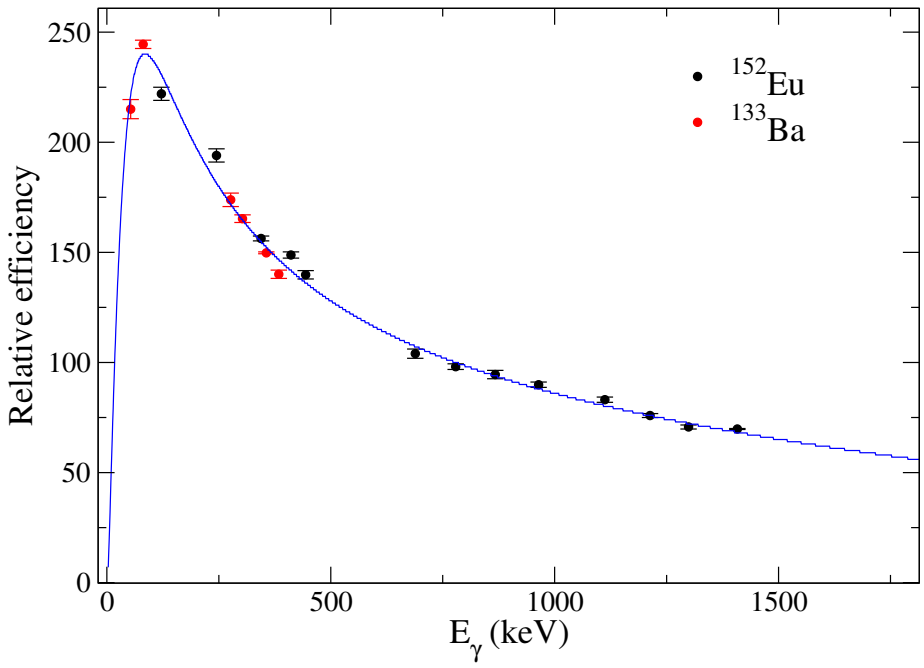

Figure 2.12 Relative efficiency vs energy plot for all the detectors of INGA set up at TIFR.

2.12.4 Data Analysis

Data sorting

To investigate nuclear structural properties, significant data sorting is necessary. To analyze a one-fold event, a one-dimensional histogram is generated with energies of transitions on one axis and the corresponding counts on the other one. This spectrum consists of all the γ peaks emitted from all the nuclei, which were populated during the deexcitation process of the compound nucleus. It is called the total projection spectrum. For the analysis of a higher-fold, higher-dimensional histogram can be generated. For the two-fold events symmetric γ - γ (4K $\times$ 4K) matrices are created, where γ-ray energies are used in both the axes, say x and y. The third axis, say z, contains the corresponding counts. With the help of γ - γ matrices, coincidence information can be obtained by choosing a slice around a certain transition energy along one axis and analyzing the projection of this slice onto

the other axis. Fig. 2.13 clarifies the concept of the coincidence method. By setting a single gate on $E2$, the coincidence spectrum shows transitions $E1$, $E3$, $E4$, $E5$, $E8$, and $E9$. If the $E1$ and $E7$ transitions are doubly gated, the gamma transitions $E6$, $E8$, and $E9$ appear in the coincidence spectrum. Similarly, cube and hypercube can be constructed for the analysis of three and four-fold data [85]. The coincidence relationship between the γ transitions are helpful in building up the level scheme of the nucleus. As high-fold histograms are constructed, the number of γ-ray events reduces due to extra-dimensional distribution and rejection of lower-fold events.

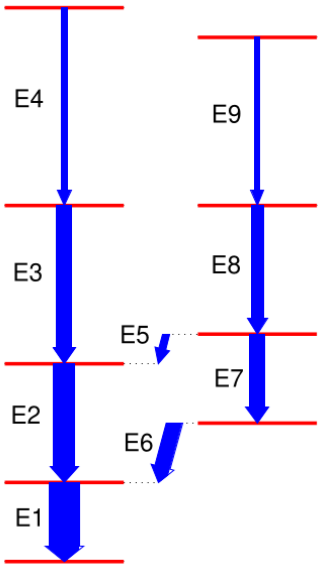

Figure 2.13 A representative partial level-scheme showing coincidence relation.

2.12.5 Angular Distribution

In heavy-ion fusion evaporation reactions, the projectile transfers orbital angular momentum to the compound nucleus. The angular momentum vector of the compound nucleus is aligned in the direction perpendicular to the projectile (beam) axis [86, 87]. The effect causes an unequal population probability $p(m_i)$ of a substate m_i. The nuclear sub-states

are preferentially populated symmetrically around $m = 0$, and the population probability $p(m_i)$ for a given spin I can be expressed as [88–90]:

$$p(m_i) = \frac{\exp\left(-m^2/2\sigma^2\right)}{\sum_{m'=-I}^{I} \exp\left(-m'^2/2\sigma^2\right)}. \tag{2.15}$$

where σ is the half-width. σ^2 (σ) is the variance (standard deviation) of the distribution, and $\sigma \to 0$ (∞) corresponds to a complete alignment (random orientation) of spin. The γ rays emitted from aligned states show characteristic angular distributions depending on their multipolarities and the spins of the involved states. In general, the angular distribution probability of multipole radiation, $W(\theta)$, when a γ radiation is emitted out in a direction θ to the beam axis, is given in terms of even powers of $\cos\theta$:

$$W_l(\theta) = \sum_{k=0}^{l} A_{2k} P_{2k}\ (cos\theta) = A_0 + A_2 P_2\ (cos\theta) + A_4 P_4\ (cos\theta) + ... + A_{2l} P_{2l}\ (cos\theta) \tag{2.16}$$

where A_{2k}'s are the angular distribution coefficients and $P(\theta)$'s are the Legendre polynomials. The coefficients A_{2k}'s depend on the degree of alignment, spins of the corresponding states, and multipole order of the transitions. The nuclei are populated in the states near yrast lines, as a result mostly dipole and quadrupole transitions are observed. For high spin decay investigations, terms beyond $k = 2$ have no significant effect on the angular distribution of the γ ray. Therefore, it is sufficient to assume terms up to second order, *i.e.*, $k = 2$.

$$W(\theta) = A_0 + A_2 P_2(\cos\theta) + A_4 P_4(\cos\theta) = A_0[1 + a_2 P_2(\cos\theta) + a_4 P_4(\cos\theta)] \tag{2.17}$$

We can obtain the angular distribution coefficients A_0, A_2, and A_4 (A_0, a_2 and a_4) by measuring the intensity of the γ-ray at different angles θ with respect to the beam axis.

The value of the angular distribution coefficients gives an idea about the multipolarity of the γ rays. For a pure dipole ($E1$ or M 1) transition, the values of the angular distribution coefficients a_2 and a_4 are -0.20 and 0, respectively, whereas the values become +0.30 and -0.10, respectively, for a pure quadrupole ($E2$ or $M2$) transitions. Mixed γ-ray transitions produce angular distribution coefficients (a_2 and a_4) that differ from pure transitions. The angular distribution of pure dipole, pure quadrupole, and mixed γ-ray transitions, along with the associated coefficients, are shown in Fig. 2.14.

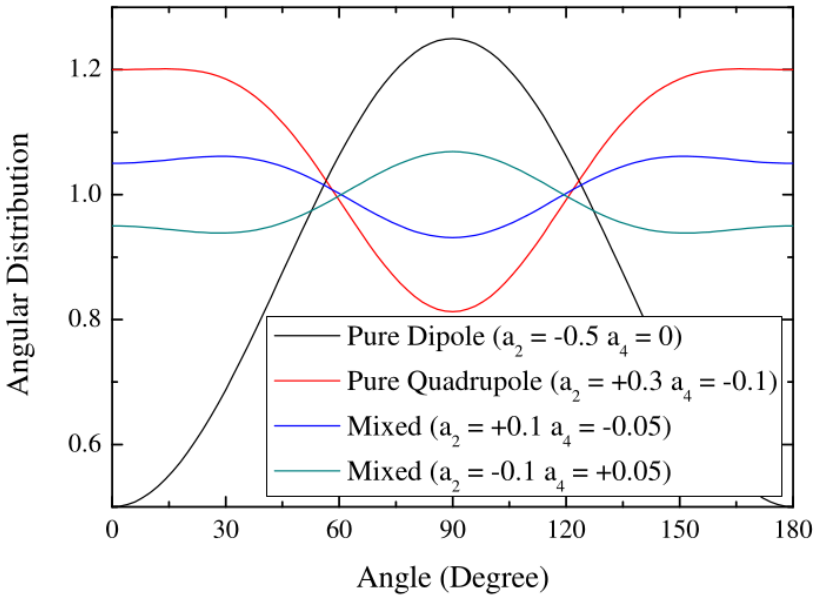

Figure 2.14 The angular distribution of pure dipole (black solid line), pure quadrupole (red solid line), and mixed (blue and olive solid lines) γ-ray transitions.

2.12.6 Mixing Ratio Calculation

The mixed transitions are generally a mixture of dipole-quadrupole or quadrupole-octupole characters, depending on the spin and parity of the states involved. The mixed transitions having ΔI = 0 or 1 is an admixture of dipole (L = 1) and quadrupole (L = 2), whereas the mixed transition with ΔI = 2 is an admixture of quadrupole (L = 2) and octupole (L

= 3). The mixing ratio of mixed gamma transitions can be calculated with the help of the standard deviation (χ^2) between the calculated and the measured angular distribution coefficients a_2 and a_4. The angular distribution coefficient of the γ transitions can be calculated theoretically by considering the partial degree of alignment as described by Yamazaki [91] and by Matelson [92]. The angular distribution coefficient for the partial alignment can be written as follows:

$$a_k = \alpha_k A_k^{max} \tag{2.18}$$

where, α is the attenuation coefficient and depends on the value of σ/j (width of sub population states). A_k^{max} is the angular distribution coefficient for fully aligned states, defined as

$$A_k^{max} = \frac{f_k(J_i L_1 L_1 J_f) + 2 * \delta f_k(J_i L_1 L_2 J_f) + \delta^2 f_k(J_i L_2 L_2 J_f)}{1+\delta^2} \tag{2.19}$$

Where J_i and J_f represent the initial and final spin of the γ-transition and L_1 and L_2 represent the possible multipolarity of γ-transition. The value of f_k can be found from the table given in Yamazaki [91] and by Matelson [92]. The standard deviation (χ^2) between the calculated and measured angular distribution coefficients a_2 and a_2 can be expressed as,

$$\chi^2 = \frac{(a_2^{exp} - a_2^{cal})^2}{3(\Delta a_2^{exp})^2} \quad + \quad \frac{(a_4^{exp} - a_4^{cal})^2}{3(\Delta a_4^{exp})^2} \tag{2.20}$$

where a_2^{exp} and a_4^{exp} represent the experimentally observed angular distribution coefficients with uncertainties Δa_2^{exp} and Δa_4^{exp} respectively. The a_2^{cal} and a_4^{cal} are the calculated angular distribution coefficients with the help of the above two equations. For the calculation of mixing ratios standard deviation χ^2 with respect to δ is plotted. If, for a particular value of δ, the standard deviation (χ^2) reaches its minimum (i.e., $\chi^2_{min} < 0.1\%$ of the

maximum deviation, χ^2_{min}), then that δ value is the measure of the mixing ratio for that transition. The uncertainty in the mixing ratio can be calculated by finding the range for which the χ^2_{min} + 1 value is reached. The $E2$ and $M1$ fractions for the mixed traditions can be calculated by $\delta^2/1+\delta^2$ and $1/1+\delta^2$ respectively.

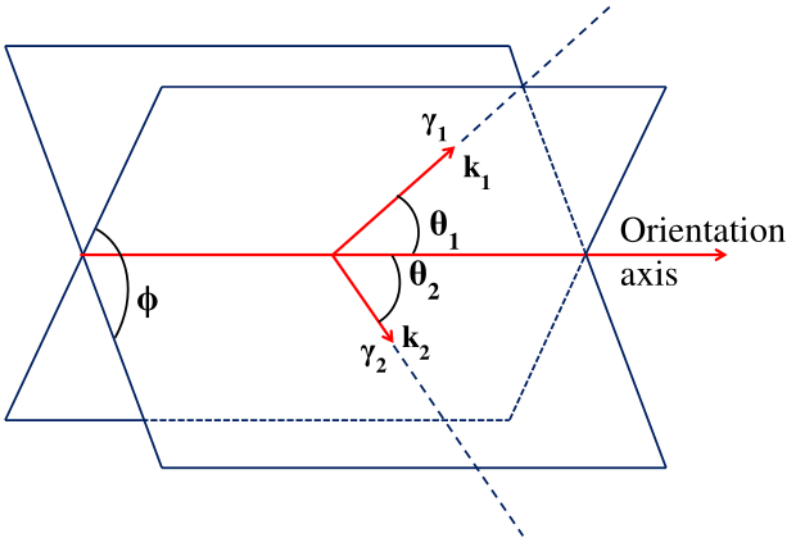

Figure 2.15 Figure shows the angles in a directional correlation of two γ transitions emitted from an oriented nucleus. ϕ is the angle between the two planes opened by each detector and the beam axis.

2.12.7 Directional Correlation (DCO) of De-exciting γ Rays

The method of directional correlation measurement is an alternative way to determine the multipole character of radiation other than angular distribution [93, 94]. Directional correlation from oriented state (DCO-ratio) is defined as the ratio of the intensities of a gamma-ray transition detected at one angle, in coincidence with another gamma-ray transition detected at a different angle (as shown in Fig. 2.15). The DCO-ratio can be expressed as,

$$R_{DCO} = \frac{I_\gamma(observed\,at\,fb,\,gate\,on\,90^\circ)}{I_\gamma(observed\,at\,90^\circ,\,gate\,on\,fb)} = \frac{I_\gamma(\gamma_1^{fb},\gamma_2^{90^\circ})}{I_\gamma(\gamma_1^{90^\circ},\gamma_2^{fb})}. \tag{2.21}$$

Here, fb represents the forward or backward angles. The term $(\gamma_1^{fb}, \gamma_2^{90^\circ})$ denote the intensity of γ_1 transition observed at forward or backward angle with gate on 90° and $(\gamma_1^{90^\circ}, \gamma_2^{fb})$ represent the intensity of γ_1 transition observed at 90° angle with gate on forward or backward angles. In order to have more statistics, the same process can be implemented with the events detected in all the detectors ($I_\gamma(all)$) taken along one of the axes. It can be defined as

$$R_\theta = \frac{I_\gamma(observed\ at\ fb,\ gate\ on\ all)}{I_\gamma(observed\ at\ 90^\circ,\ gate\ on\ all)} = \frac{I_\gamma(\gamma_1^{fb}, \gamma_2^{all})}{I_\gamma(\gamma_1^{90^\circ}, \gamma_2^{all})}. \tag{2.22}$$

2.12.8 Width of Sub-State Population (σ/j)

The sub-state population (σ/j) width plays an important role in determining the multi-polarity of the γ rays decaying from the oriented nuclei. In equation 2.15, the sub-state population parameter $p(m_i)$ is represented, which shows a Gaussian distribution centered around $m = 0$ for a given J. The quantity (σ/j) represents the width of the sub-state population and remains constant over a wide range of given spins. A variation from this empirical fact happens exclusively in the low-spin region I$\leq$6. To estimate the value of (σ/j), pure dipole (mostly $E1$) transitions are selected, and their R_{DCO} values are measured by gating on stretched $E2$ transitions. The theoretical value of R_{DCO} can be calculated with the help of the ANGCOR [95] program by varying (σ/j). The experimentally observed DCO ratios then have to be compared with theoretical values of R_{DCO} to obtain the (σ/j) value. The average of the (σ/j) for the selected $E1$ transitions indicates the width of the sub-state population in a specific reaction. This value is then used in the calculation of mixing ratios of the γ transition emitted from the nuclei in the given reaction. In Fig. 2.16, a comparison between the experimental and calculated values R_{DCO} at different value of (σ/j) is shown, which gives $(\sigma/j) \approx 0.31$ for the reaction ^{109}Ag(^{13}C, 3n)^{119}I.

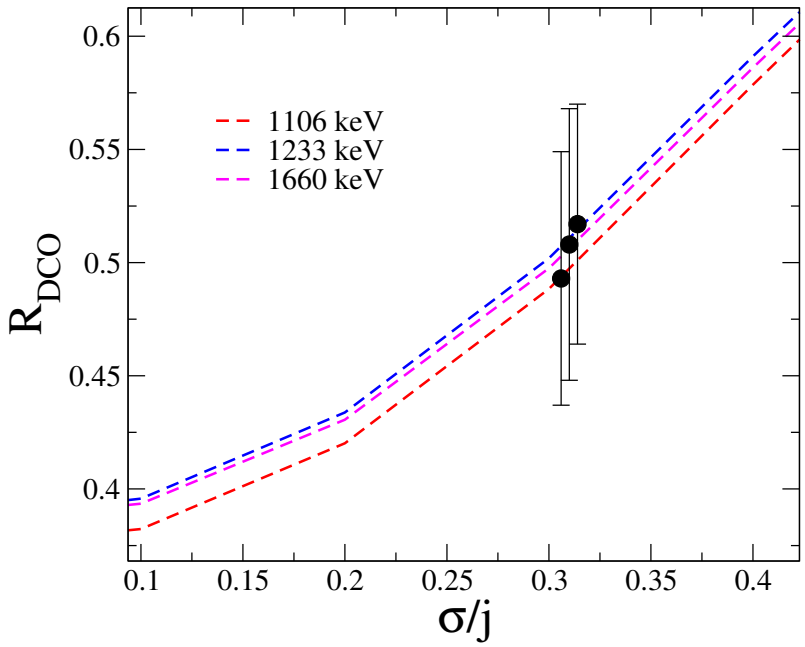

Figure 2.16 Figure shows the comparison between the experimental and calculated values of R_{DCO} at different value of (σ/j).

2.13 Linear Polarization of γ transitions

In heavy ion fusion evaporation reactions, the measurement of DCO and ADO ratios only gives the idea about the multipolarity of γ-transitions. The electromagnetic character (the electric or magnetic type) of γ rays can be determined by combining the DCO and ADO ratios analysis results with the linear polarization measurements [96, 97].

The linear polarization of the γ-ray transitions emitted from the oriented states closely complies the angular distribution of these γ rays. When γ rays are linearly polarized, the angular distribution function of γ rays depends not only on their outgoing direction θ with respect to the beam axis but also on their electric field direction ε (Fig. 2.17) with respect to the reaction plane (defined by the beam axis and the outgoing direction of γ-rays). The angular distribution of linearly polarized γ rays emitted from axially oriented nuclei is

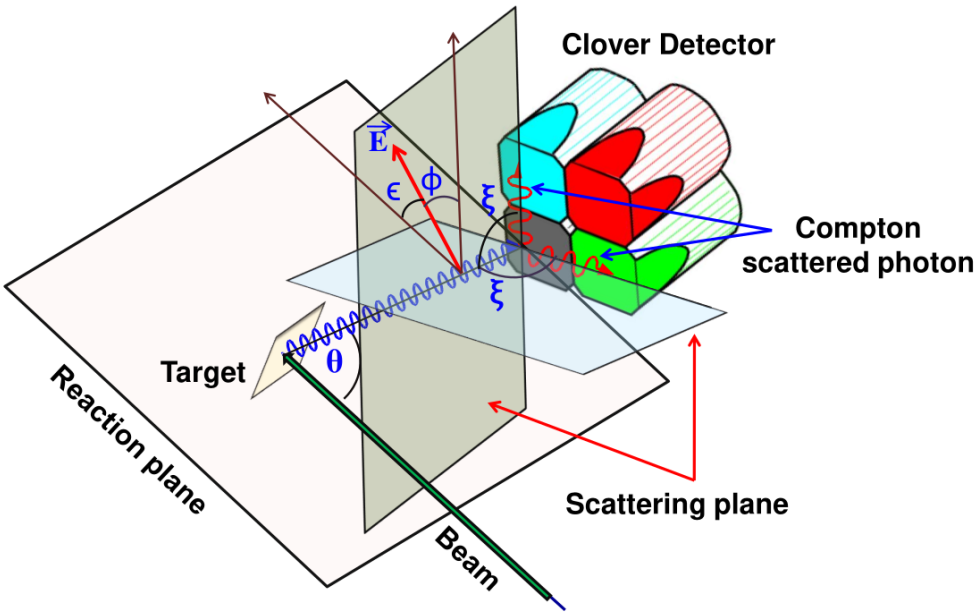

Figure 2.17 Figure shows the use of a clover detector as a Compton polarimeter [71]. The explanations of the relevant angles $(\theta, \varepsilon, \phi$, and $\zeta)$, shown in the above figure, are given in the text.

given by [98]:

$$W(\theta,\phi) = \frac{d\Omega}{8\pi} \sum_{\lambda=even} B_\lambda U_\lambda [A_\lambda P_\lambda(cos\theta) + 2A_{\lambda,2} P_\lambda^{(2)}(cos\theta) cos2\phi], \tag{2.23}$$

Where ϕ is the angle between the electric vector and the scattering plane. B_λ are orientation tensors and U_λ are de-orientation coefficients.

The linear polarization of photons can be determined by taking the normalized difference in the number of photons occupying two polarization states. Therefore, the linear polarization of γ rays can be expressed in terms of the angular distribution by considering the electric field $W(\theta, \varepsilon = 0^\circ)$ in the reaction plane and perpendicular to it $W(\theta, \varepsilon = 90^\circ)$.

$$P(\theta) = \frac{W(\theta,\phi = 0^\circ) - W(\theta,\phi = 90^\circ)}{W(\theta,\phi = 0^\circ) + W(\theta,\phi = 90^\circ)} \tag{2.24}$$

The values of $P(\theta)$ lie between ± 1. For completely polarized γ-rays, the value of $P(\theta)$ will be 1, whereas for unpolarized γ-rays $P(\theta)$ will be 0. During the time of the experiment, 90° angles are selected for the polarization measurement because the magnitude of $P(\theta)$ is maximum at 90°. Using equations 2.19 and 2.23, equation 2.24 can be written as,

$$P_{cal}(90^\circ) = \pm \frac{3a_2H_2 - 7.5a_4H_4}{2 - a_2 + 0.75a_4} \tag{2.25}$$

Where a_2 and a_4 represent the angular distribution coefficient, and the +(-) sign applies for a transition without (with) parity change. The H_2 and H_4 are the polarization parameters and depend on the initial and final spin and the mixing ratio δ. For pure $M1$ and $E1$ transitions, the value of H_2 is 1 and H_4 is -1/6. for mixed transitions, the value of H_4 remains the same, and the value of H_2 defined as

$$H_2(L=1,L'=2) = \frac{F_2(11) - 0.667\delta F_2(12) + \delta^2 F_2(22)}{F_2(11) + 2\delta F_2(12) + \delta^2 F_2(22)} \tag{2.26}$$

where the coefficient $F_2(L=1,L'=2)$ can be obtained from the Ref. [91]. With the help of the equations 2.25 and 2.26, the linear polarization as a function of a_2 and a_4 can be expressed as:

$$\begin{aligned} P(\theta)_{E1} &= -\frac{3a_2 \sin^2\theta}{2 - a_2 + 3a_2\cos^2\theta} \\ P(\theta)_{M1} &= \frac{3a_2 \sin^2\theta}{2 - a_2 + 3a_2\cos^2\theta} \end{aligned} \tag{2.27}$$

$$P(\theta)_{E2} = 3a_2 \sin^2\theta + a_4[(35/4)cos^4\theta - 10cos^2\theta + (5/4)] \times \frac{1}{A} \tag{2.28}$$

where,

$$A = 2 - a_2 + 3a_2\cos^2\theta + a_4[(35/4)cos^4\theta - (30/4)cos^2\theta + (3/4)]$$

At $\theta = 90^\circ$, the value of the above multipolarity γ transition is given by:

$$\begin{aligned} P(\theta)_{E1} &= -\frac{3a_2}{2-a_2} \\ P(\theta)_{M1} &= \frac{3a_2}{2-a_2} \\ P(\theta)_{E2} &= \frac{3a_2+1.25a_4}{2-a_2+0.75a_4} \\ P(\theta)_{M2} &= -\frac{3a_2+1.25a_4}{2-a_2+0.75a_4} \end{aligned} \tag{2.29}$$

From the above equations, the sign of magnetic and electric transitions can be determined. For the pure dipole transition, the value of a_2 is negative and the a_4 value is zero. Hence, electric dipole transitions have a positive value of linear polarization, and magnetic dipole transitions have a negative value. On the other hand, the value of a_2 is positive and a_4 is negative for quadrupole transitions, so $P(\theta)$ has a positive value for electric quadrupole transitions and a negative value for magnetic quadrupole transitions. In the case of mixed transition, the value of linear polarization is close to zero.

2.13.1 Experimental Method of Linear Polarization Measurement

In γ-ray spectroscopy, Compton scattering is an effective technique to measure the experimental value of linear polarization. The differential cross-sections of the γ- rays with an energy of E_γ can be obtained by the Klein-Nishina formula [99]

$$\sigma(\xi,\phi) = \frac{d\sigma}{d\Omega}(\xi,\phi) = \frac{r_0^2}{2}\left(\frac{E_\gamma}{E'_\gamma}\right)^2\left[\frac{E_\gamma}{E'_\gamma}+\frac{E'_\gamma}{E_\gamma}-2\sin^2\xi\cos^2\phi\right] \tag{2.30}$$

Where E'_γ represents the scattered photon energy. ξ is the Compton scattering angle with respect to the incident γ -ray direction and ϕ is the angle between the Compton scattering plane and the polarization plane of the incoming radiation (as shown in Fig. 2.17). Here, r_0 represents the classical radius of electron which is equal to $e^2/m_e c^2$ with

m_e is the mass of the electron. From the above equation, it is clear that the differential cross section becomes maximum when ϕ is 90°, *i.e.*, in the direction perpendicular to the electric field vector. Hence, the radiation power emitted becomes maximum in a direction perpendicular to the axis of electric dipole oscillation.

The use of Clover detectors in an INGA setup enables linear polarization detection of γ radiation, a useful technique for discriminating between electric and magnetic transitions. The four crystals of clover detectors are used as Compton polarimeters. Each crystal of a clover detector acts as a scatterer, and the two adjacent crystals act as an analyzer. Since linear polarization has a maximum value at 90°, mostly 90° detectors are used for this purpose. The list mode data was sorted to discriminate Compton scattered events (both horizontally and vertically dispersed with respect to the reference plane) in adjoining pairs of Ge crystals in clover detectors. For the measurement of polarization, two $E_\gamma - E_\gamma$ matrices were created with either horizontally or vertically scattered γ-rays (at 90° detectors) on one axis and coincident γ-rays from all the detectors on the second axis. Now, linear polarization (P) is experimentally defined as the ratio of polarization asymmetry (Δ) and polarization sensitivity (Q) and can be expressed as follows:

$$P = \frac{\Delta}{Q(E_\gamma)} \tag{2.31}$$

where Δ represents polarization asymmetry and is defined as the ratio of the normalized difference of the perpendicular and parallel scattered photons to their sum [96].

$$\Delta_{asym} = \frac{a(E_\gamma)N_\perp - N_\parallel}{a(E_\gamma)N_\perp + N_\parallel} \tag{2.32}$$

where $N_\perp$ and $N_\parallel$ are the numbers of scattered photons in a direction perpendicular and parallel to the direction of the reaction plane. $a(E_\gamma)$ represents the correction factor, which

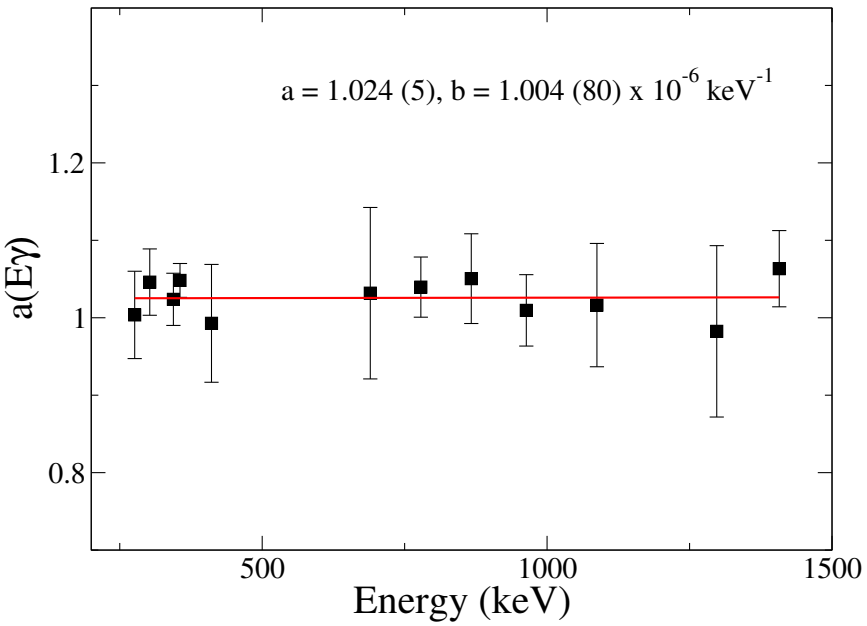

Figure 2.18 Figure shows the asymmetry correction factor at different energies of γ transitions.

describes the geometrical asymmetry of the detection system and is defined as [96, 97]:

$$a(E_\gamma) = \frac{N_{\parallel}}{N_{\perp}} \mid_{unpolarized} \tag{2.33}$$

This can be evaluated by using γ rays of known unpolarized radioactive sources (^{152}Eu, ^{133}Ba) for which a value close to unity is obtained (see Fig. 2.18). The values of Δ_{asym} can be positive or negative depending on the type of transition (electric or magnetic). A number close to zero suggests mixing.

The polarization sensitivity Q is a parameter to characterize a Compton polarimeter and depends on the Compton scattering angle ξ and the incident photon energy E_γ. According to Ref. [100] sensitivity Q can be defined as a linear function given as:

$$Q = Q_0(a + bE_\gamma) \tag{2.34}$$

Q_0 defines the sensitivity of a point-like absorber placed at a scattering angle $\xi = 90^\circ$ and is represented as:

$$Q_0 = \frac{1+\alpha}{1+\alpha+\alpha^2} \tag{2.35}$$

with $\alpha = \frac{E_\gamma(keV)}{511}$. Once the sensitivity as a function of the incident γ-ray energy is known, the linear polarization of the γ rays can be directly found by using the asymmetry measurement. The value of sensitivity increases as the distance between a scatterer and an absorber increases because the solid angle decreases, but due to a decrease in the solid angle, the coincidence efficiency becomes lower. Thus, the overall quality of a Compton polarimeter depends on both coincidence efficiency as well as sensitivity [101].

2.13.2 Mixing Ratio Calculation via R_{DCO} -Polarization Method

This method is an alternative to the angular distribution method for determining the mixing ratio of γ-transitions. In this method, the theoretical value of R_{DCO} and linear polarization are calculated by varying δ within a range of -50 to 50, having intervals. The theoretical value of R_{DCO} is calculated by using the ANGCOR code [95], and the theoretical value of polarization can be calculated by using equations 2.25 and 2.26. Then a contour plot of R_{DCO} and polarization is obtained for different values of δ. The experimental value of R_{DCO} and polarization of the observed transition are then compared with the theoretical values. To observe the value of δ, the standard deviation χ^2 values (between the measured and calculated values) are plotted with respect to δ, and then that value of δ is considered for which the χ^2 is minimum.